

Contribution from the Department of Chemistry & Institute for Materials Research, McMaster University, Hamilton, Ontario, Canada L8S 4M1, and Department of Chemistry, University of Toronto, Toronto, Ontario, Canada M5S 1A1

Crystal Structure and ^{127}I Mössbauer Spectrum of Diphenyliodonium-2-carboxylate Hydrate, $\text{C}_{13}\text{H}_9\text{IO}_2 \cdot \text{H}_2\text{O}$: Secondary vs. Hydrogen Bonding

Raymond J. Batchelor,[†] Thomas Birchall,^{*†} and Jeffery F. Sawyer^{*†}

Received August 20, 1985

The crystal and molecular structure of diphenyliodonium-2-carboxylate, $\text{C}_6\text{H}_5\text{IC}_6\text{H}_4\text{-o-CO}_2\text{H}_2\text{O}$, has been determined. Crystals are monoclinic, of space group $P2_1/n$, with $a = 10.469$ (1) Å, $b = 10.407$ (5) Å, $c = 14.004$ (3) Å, $\beta = 127.74$ (2)°, $V = 1206.5$ Å³, $D_c = 1.88$ g cm⁻³ for $Z = 4$, and $R_1 = 0.0319$ ($R_w = 0.0438$) for 2123 observed ($I > 3\sigma(I)$) reflections. The geometry about iodine consists of primary bonds to the two phenyl rings ($\text{I-C} = 2.105$ (4) and 2.119 (4) Å) and a weak primary bond or strong intramolecular secondary I-O bond of length 2.478 (4) Å to the *o*-carboxylate group in an approximate trigonal-bipyramidal AX_3E_2 arrangement. The C-I-C angle (95.2 (1)°) has opened to accommodate the I-O interaction and to reduce a $\text{C}\cdots\text{H}$ interaction of 2.56 (4) Å between the phenyl rings. Unexpectedly, no further $\text{I}\cdots\text{O}$ secondary bonding occurs and the crystal packing is dictated by hydrogen bonds involving the water molecule in the lattice. The ^{127}I Mössbauer spectrum of the title compound has been recorded, and the data have been used to estimate an I-O bond valency that is in agreement with that obtained from the crystallographic data. Details of the preparation of a $\text{Ca}_3^{127\text{m}}\text{TeO}_6$ source for ^{127}I Mössbauer spectroscopy are reported.

Introduction

Recently, there has been significant interest in the directional preferences of the inter- and intramolecular charge-transfer or secondary bonding interactions in compounds of the non-metals. These interactions are significantly shorter than van der Waals distances but are normally much longer than primary bond lengths.¹ In particular, the arrangements of such contacts involving the elements Sn(IV), S(II), As(III), and Sb(III) have been reviewed.²⁻⁶ For I(III), Etter⁷ and Gougoutas⁸ have commented on the persistent geometry of several weak $\text{I(III)}\cdots\text{O}$ interactions in compounds containing the benziodoxole nucleus and the role they play in photochemical reactions, and others⁹⁻¹¹ have noted three main arrangements of primary and secondary bonds involving I(III). These are the square-planar arrangements of two primary and two secondary bonds (an $\text{AX}_2\text{Y}_2\text{E}_2$ geometry—see ref 6 for notation) or three primary bonds and one secondary bond (an $\text{AX}_3\text{Y'E}_2$ geometry) and an approximately pentagonal-planar arrangement of three primary and two secondary bonds (an $\text{AX}_3\text{Y}_2\text{E}_2$ geometry). The present structure was determined to gain further information on $\text{I}\cdots\text{O}$ secondary bonds.

Experimental Section

X-ray Crystallography. Crystals (Alfa Chemical Co.) were well-formed white needles. Precession photographs were used to check crystal quality and to obtain preliminary cell and symmetry information. Further work using a needle-shaped crystal with faces (011), (0 $\bar{1}\bar{1}$), (10 $\bar{1}$), ($\bar{1}01$), (01 $\bar{1}$), and (0 $\bar{1}\bar{1}$) 0.004, 0.004, 0.005, 0.005, 0.020, and 0.020 cm from an origin within the crystal on an Enraf-Nonius CAD-4 diffractometer with graphite-monochromatized Mo $K\alpha$ radiation ($\lambda = 0.71069$ Å) gave the crystal data in Table I. Intensity data were collected by using ω - 2θ scans over scan ranges (0.80 + 0.35 tan θ)°. Scan rates were selected to give $I/\sigma(I) \geq 25$ within a maximum scan time of 85 s. Backgrounds obtained by extending the scan by 25% on either side of peak were measured for half the time taken to collect the peak. All (3822) reflections in the quadrant ($h, k, \pm l$) with $2\theta < 55^\circ$ were collected. Three standard reflections measured every 7500 s of exposure time showed a slight decomposition of the crystal. Lorentz, polarization, and absorption corrections (program ABCOR,¹² $8 \times 10 \times 10$ grid, minimum transmission factor 0.769, maximum transmission factor 0.828) and corrections for crystal decay (maximum rescale factor (on F) 1.173) were applied to all reflections. Zero F_o data and systematically absent reflections (378) were excluded, and 340 symmetry-equivalent data were then averaged ($R_{\text{merge}}(F) = 0.022$) to give a final data set of 2360 unique reflections.

Structure solution: Patterson for iodine; least-squares, Fourier,* and difference Fourier methods for all remaining atoms. Full-matrix least squares minimizing $w\|F_o - |F_c|\|^2$ then converged (maximum $\Delta/\sigma = 0.05$) to final agreement indices $R_1 = 0.0319$ ($R_w = 0.0438$) for 2123 reflections with $I > 3\sigma(I)$. In prior cycles the water hydrogen atom positions

Table I. Crystal Data

compd	$\text{C}_{13}\text{H}_{11}\text{IO}_3$
syst	monoclinic
$a \times b \times c$, Å	10.469 (1) × 10.407 (5) × 14.004 (3)
β , deg	127.74 (2)
V , Å ³	1206.5
f_w	342.1
Z	4
D_{calcd} , g cm ⁻³	1.88
$F(000)$	664
$\mu(\text{Mo } K\alpha)$, cm ⁻¹	26.2
space group	$P2_1/n$
T , °C	23
no. of reflctns used in cell dtn	25 ($8.1 < \theta < 16.7^\circ$)

Table II. Positional Parameters and Their Estimated Standard Deviations^a

atom	x	y	z	B , Å ²
I	0.53269 (3)	0.23460 (3)	0.41428 (2)	3.861 (6)
O1	0.4853 (4)	0.2639 (3)	0.5660 (3)	4.93 (7)
O2	0.5635 (3)	0.3918 (4)	0.7194 (2)	5.15 (7)
O3	0.2330 (4)	0.0747 (4)	0.4685 (3)	7.3 (1)
C1	0.6901 (3)	0.3838 (4)	0.5303 (3)	3.19 (8)
C2	0.7912 (4)	0.4427 (4)	0.5121 (3)	3.84 (9)
C3	0.8916 (4)	0.5382 (4)	0.5905 (3)	4.3 (1)
C4	0.8907 (4)	0.5745 (4)	0.6843 (3)	4.5 (1)
C5	0.7875 (4)	0.5141 (4)	0.7003 (3)	3.97 (9)
C6	0.6839 (4)	0.4183 (4)	0.6230 (3)	3.35 (8)
C7	0.6074 (4)	0.2367 (4)	0.3047 (3)	3.53 (8)
C8	0.7244 (4)	0.1503 (5)	0.3304 (3)	4.3 (1)
C9	0.7773 (4)	0.1538 (6)	0.2604 (3)	5.3 (1)
C10	0.7148 (5)	0.2384 (4)	0.1696 (4)	4.9 (1)
C11	0.5957 (5)	0.3224 (5)	0.1426 (3)	5.0 (1)
C12	0.5401 (4)	0.3233 (4)	0.2108 (3)	4.2 (1)
C13	0.5702 (4)	0.3542 (4)	0.6398 (3)	3.80 (9)
H1	0.785 (3)	0.419 (4)	0.449 (3)	4 (1)*
H2	0.949 (3)	0.575 (5)	0.581 (3)	5 (1)*
H3	0.952 (4)	0.634 (4)	0.725 (3)	4.4 (9)*
H4	0.785 (3)	0.531 (4)	0.759 (2)	4 (1)*
H5	0.764 (4)	0.094 (4)	0.389 (3)	5 (1)*
H6	0.860 (4)	0.099 (4)	0.281 (3)	5 (1)*
H7	0.740 (5)	0.231 (4)	0.110 (4)	6 (1)*
H8	0.539 (4)	0.384 (4)	0.070 (3)	5 (1)*
H9	0.451 (4)	0.388 (4)	0.187 (3)	5 (1)*
H10	0.183 (3)	0.085 (4)	0.400 (3)	3.6 (9)*
H11	0.289 (5)	0.115 (5)	0.489 (3)	11 (1)*

^a Starred values indicate that the atoms were refined isotropically. Anisotropically refined atoms are given in the form of the equivalent isotropic thermal parameter defined as $\frac{1}{3}[a^2\beta(1,1) + b^2\beta(2,2) + c^2\beta(3,3) + ab(\cos \gamma)\beta(1,2) + ac(\cos \beta)\beta(1,3) + bc(\cos \alpha)\beta(2,3)]$.

[†] McMaster University.
[†] University of Toronto.

were found to oscillate and were fixed in the final cycles of least squares. Weights in the final cycle of refinement were given by $w = 4F^2[\sigma^2(I) +$

Table III. Bond Distances (Å), Bond Angles (deg) and Least-Squares Mean Planes

Bond Lengths					
I-C1	2.119 (4)	C1-C2	1.376 (5)	C7-C8	1.378 (6)
I-C7	2.105 (4)	C1-C6	1.385 (5)	C7-C12	1.381 (6)
I-O1	2.478 (4)	C2-C3	1.374 (6)	C8-C9	1.390 (6)
O1-C13	1.272 (4)	C3-C4	1.372 (6)	C9-C10	1.343 (7)
O2-C13	1.223 (4)	C4-C5	1.382 (6)	C10-C11	1.372 (8)
O3-H10	0.77	C5-C6	1.380 (5)	C11-C12	1.390 (6)
O3-H11	0.63	C6-C13	1.504 (5)		
		C-H	0.79 (4)–1.03 (4)		
Bond Angles					
C1-I-C7	95.2 (1)	C2-C3-C4	121.0 (4)	C8-C7-C12	121.9 (4)
C1-I-O1	73.9 (1)	C3-C4-C5	119.6 (4)	C7-C8-C9	118.2 (4)
C7-I-O1	169.0 (1)	C4-C5-C6	121.2 (4)	C8-C9-C10	120.8 (5)
I-O1-C13	112.4 (3)	C1-C6-C5	117.3 (4)	C9-C10-C11	120.8 (5)
I-C1-C2	120.6 (3)	C1-C6-C13	121.8 (3)	C10-C11-C12	120.5 (4)
I-C1-C6	116.6 (3)	C5-C6-C13	121.0 (3)	C7-C12-C11	117.8 (4)
C2-C1-C6	122.7 (4)	I-C7-C8	118.1 (3)	O1-C13-O2	125.2 (4)
C1-C2-C3	118.2 (4)	I-C7-C12	120.1 (3)	O1-C13-C6	115.3 (3)
				O2-C13-C6	119.5 (4)
		H10-O3-H11	101	C-C-H	114 (3)–126 (3)
Mean Planes and Deviations from Plane (Å) ^{a,b}					
-0.4360x + 0.6773y - 0.5926z = 1.9393					
I* -0.0060 (4), C1* 0.001 (4), C2* 0.005 (4), C3* 0.000 (4), C4* -0.005 (4), C5* -0.005 (4), C6* 0.010 (4), C7 -0.023 (4), C10 -0.119 (5), O1 -0.012 (3), O2 0.100 (3), O3 0.080 (4), C13 0.029 (4), H1 0.05 (4), H2 0.03 (4), H3 0.02 (4), H4 0.04 (4)					
-0.4049x - 0.6666y - 0.6258z = -5.2620					
I 0.0560 (4), C7* -0.008 (4), C8* 0.007 (4), C9* 0.000 (5), C10* -0.008 (5), C11* 0.007 (5), C12* 0.001 (4), H5 0.03 (4), H6 -0.04 (4), H7 0.15 (5), H8 0.07 (4), H9 0.01 (4)					

^a Atoms defining the plane are marked with asterisks. ^b Angle between planes 87.8°.

(0.05F²)⁻¹. At convergence, the esdow was 1.21 e, and a final difference Fourier contained a few peaks up to 1.31 e Å⁻³ in height close to the iodine. Programs: Enraf-Nonius SDP package¹² on a PDP 11/23 computer. Scattering factors and *f'* and *f''* corrections were stored in program. The final positional and thermal parameters and bond lengths/bond angles are given in Tables II and III.

Mössbauer Spectroscopy. The source of 57.6-keV γ radiation was Ca₃^{127m}TeO₆. The use of calcium tellurate as a source matrix for ¹²⁹I Mössbauer spectroscopy has been previously reported.¹³ Our source was prepared by irradiating 0.5 g of 98%-enriched ¹²⁶TeO₂ in a quartz vial, in graphite reflector elements on the edge of the reactor core at a nominal thermal neutron flux of 1.5 × 10¹³ cm⁻² s⁻¹ for approximately 4 months. The McMaster University nuclear reactor is a 5-MW (thermal) pool-type reactor. The estimated activity of ^{127m}Te produced is ~5 mCi. Note, however, that only 0.8% of ^{127m}Te decays populate the 57.6-keV level of ¹²⁷I.¹⁴

The irradiated TeO₂ was then dissolved in concentrated aqueous ammonia containing 1.5 cm³ of 30% hydrogen peroxide with gentle warming for 20 min. Calcium oxide, 0.061 g (15% excess), was then added, and the mixture was boiled under reflux for 24 h. After the mixture was cooled to room temperature, the insoluble Ca₃TeO₆ was contained, by suction filtration of the mixture through a disk of Whatman 42 filter paper, in a specially machined, perforated, Delrin plastic tapered capsule that was seated in a tapered ground-glass section in the neck of a Pyrex funnel. The active Ca₃TeO₆ was compressed into the plastic capsule

contained inside a threaded aluminum cell. Apiezon-N grease was applied to the threads of the cell and to the cap of the plastic capsule to ensure against leakage. (No external radioactive contamination was observed after repeated immersion in liquid helium.) The minimum wall thickness of the aluminium cell was 2 mm, sufficient to effectively eliminate the β radiation from the source.

Dry-run tests of this process had already been performed on inactive TeO₂ containing the natural isotopes, and these tests showed that the filtrate contained no tellurium. The precipitate was an amorphous white powder for which no X-ray powder diffraction pattern was observable with Cu K α radiation. When a stoichiometric amount of CaO was used in the preparation, the solid product was found to contain 37.2% Te (37.1% calculated for Ca₃TeO₆).

An alternative and experimentally easier procedure would be the preparation of nonradioactive Mg₃¹²⁶TeO₆, which could then be irradiated repeatedly to generate the ^{127m}Te activity as has been reported for the generation of the ^{129m}Te source.¹⁵ One advantage of performing the chemistry after irradiation, as we have done, is to eliminate the possibility of radiation damage to the source matrix arising from the longer irradiation times required to generate sufficient ^{127m}Te. We hope in the future to investigate the relative qualities of sources prepared by these two different methods.

With the amorphous Ca₃TeO₆ source at 4.2 K, the spectrum of cuprous iodide (4.2 K) (0.015 g cm⁻² of ¹²⁷I) displayed a perfectly Lorentzian single line with fwhm = 3.75 (6) mm s⁻¹. This is, within error, identical with the signal obtained for the same absorber but by using a commercial source of Zn^{127m}Te from New England Nuclear Corp. The dependence of line width on CuI absorber thickness appears to be linear in the range 0.015–0.075 g cm⁻² ¹²⁷I and extrapolates to fwhm = 3.04 mm s⁻¹ for an infinitesimal sample thickness (2 Γ_{127} (theor) = 2.54 mm s⁻¹). By comparison, the ¹²⁹I Mössbauer line width for CuI extrapolated to infinitesimal thickness, by using a Mg₃^{129m}TeO₆ source,¹³ was 0.7 mm s⁻¹ (2 Γ_{129} (theor) = 0.59 mm s⁻¹). This implies that the amorphous Ca₃TeO₆ source also contains Te in a cubic local environment. Measurement of the recoilless fraction for amorphous Ca₃TeO₆ was omitted because of the high background count rate, which was a consequence of the use of a scintillation detector and the intense 28-keV X-ray occurring in the γ spectrum of ^{127m}Te. This background was reduced as much as possible by the use of a lead filter 0.05 mm thick.

The sample of C₆H₅IC₆H₄CO₂·H₂O was finely ground and pressed into a threaded Kel-F cell to give 0.05 g cm⁻² of ¹²⁷I. ¹²⁷I Mössbauer spectra were recorded with both source and absorber immersed in liquid He in a cryostat manufactured by Janis Corp. An Elscint MFG-N-5 Mössbauer function generator, an Elscint MDF-N-5 driver/generator, and an Elscint MVT-4 transducer operating in the constant-acceleration

- (1) Alcock, N. W. *Adv. Inorg. Chem. Radiochem.* **1973**, *15*, 1.
- (2) Britten, D.; Dunitz, J. D. *J. Am. Chem. Soc.* **1981**, *103*, 2971.
- (3) Guru-Row, T. N.; Parthasarathy, R. *J. Am. Chem. Soc.* **1981**, *103*, 477.
- (4) Rosenfield, R. E.; Parthasarathy, R.; Dunitz, J. D. *J. Am. Chem. Soc.* **1977**, *99*, 4860.
- (5) Perlik, F. *Montash. Chem.* **1979**, *110*, 387.
- (6) Sawyer, J. F.; Gillespie, R. J. *Prog. Inorg. Chem.*, in press.
- (7) Etter, M. C. *J. Solid State Chem.* **1976**, *16*, 399.
- (8) Gougoutas, J. Z.; Clardy, J. C. *J. Solid State Chem.* **1972**, *4*, 226.
- (9) Alcock, N. W.; Countryman, R. M.; Esperas, S.; Sawyer, J. F. *J. Chem. Soc., Dalton Trans.* **1979**, 854.
- (10) Birchall, T.; Myers, R. D. *J. Am. Chem. Soc.* **1981**, *103*, 2971; *J. Chem. Soc., Dalton Trans.* **1983**, 885.
- (11) Archer, E. M.; van Schalkwyk, G. D. *Acta Crystallogr.* **1953**, *6*, 88.
- (12) *Enraf-Nonius Structure Determination Package*; B. A. Frenz: College Station, TX, 1981.
- (13) Pasternak, M.; Van der Heyden, M.; Langouche, G. *Nucl. Instrum. Methods Phys. Res., Sect. B* **1984**, *232* [B4], 152.
- (14) Lederer, C. M.; Hollander, J. M.; Perlman, I. *Table of the Isotopes*, 6th ed.; Wiley: New York, 1967; p 271.

Table IV. Primary and Secondary Bond Distances in Organoiodine(III) Compounds^{a-c}

compd	a, Å	b, Å	c, Å	d, Å	e, Å	f, Å	ref
1	2.08	2.11	2.768	3.089			23
2	<u>2.128</u>	1.952	2.286	2.941			d
	2.136	1.952	2.284	3.031			d
3	<u>2.083</u>	1.940	2.473	3.003	3.351		e
4	2.16	2.00	2.30	2.90			22
5	2.10	2.46 (Cl)	2.10	nca ^f			26
6	2.09	2.52 (Cl)	2.14	nca ^f			26
7	2.119	2.105	2.478	none			j
8	<u>2.090</u>	2.159	2.153	2.817	2.850		9
9a	<u>2.083</u>	2.163	2.136	2.936	2.936	3.049	9
9b	<u>2.074</u>	2.186	2.138	3.000	3.038	3.133	g
10a	<u>2.078</u>	2.096	3.105 (Cl)	3.064 (Cl)			20
10b	<u>2.071</u>	<u>2.095</u>	3.248 (Br)	3.253 (Br)			20
10c	<u>2.095</u>	<u>2.103</u>	3.453 (I)	3.453 (I)			20
10d	<u>2.114</u>	<u>2.114</u>	2.768	2.877			17
10e	<u>2.02</u>	<u>2.05</u>	2.94 (F)	2.96 (F)			19
11	<u>2.089</u>	<u>2.078</u>	3.166	3.138	2.966 (N)	3.287 (N)	24
12	2.00	2.45 (Cl)	2.45 (Cl)	3.40 (Cl)			11
13	<u>2.06</u>	1.96	2.33	3.01	3.02		h
	2.05	2.05	2.31	3.00	3.00		h
14	2.104	2.234 (B)	3.664 (I)	3.497 (I)			18
	2.111	2.261 (B)	3.718 (I)	3.464 (I)			18
15	<u>2.053</u>	nca ^f	2.770	3.419 (F)			i

^a See also ref 8. ^b Bonds underlined are to carbon. Other bonds are to oxygen unless otherwise indicated. ^c van der Waals radii (Å): I, 2.15; Br, 1.95; Cl, 1.80; F, 1.35; O, 1.40; N, 1.5. ^d Balthazor, T. M.; Miles, J. A.; Stults, B. R. *J. Org. Chem.* **1978**, *43*, 4538. ^e Koser, G. F.; Wettach, R. H. Troup, J. M.; Frenz, B. A. *J. Org. Chem.* **1976**, *41*, 3609. ^f nca = no coordinates available. ^g Stergioudis, G. A.; Kokkou, S. C.; Bozopoulos, A. P.; Rentzepis, P. J. *Acta Crystallogr., Sect. C: Cryst. Struct. Commun.* **1984**, *C40*, 877. ^h Alcock, N. W.; Countryman, R. M. *J. Chem. Soc., Dalton Trans.* **1979**, 851. ⁱ Moriarty, R. M.; Prakash, I.; Prakash, O.; Freeman, W. A. *J. Am. Chem. Soc.* **1984**, *106*, 6082. ^j This work.

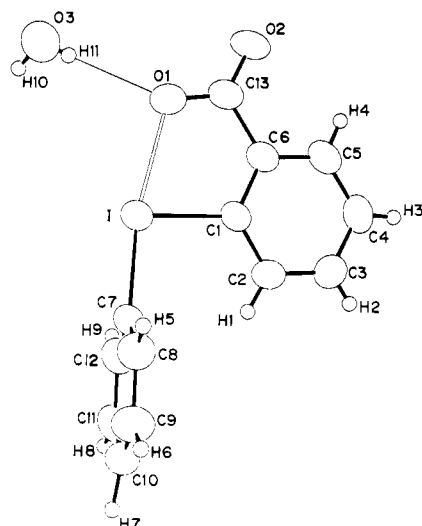


Figure 1. ORTEP view of the molecule showing the atomic numbering scheme, the intramolecular I-O interaction, and one of the hydrogen bonds. Thermal ellipsoids are drawn at the 50% probability level.

triangular-waveform mode were used. A NaI(Tl) (6.35-mm) scintillation counter (Harshaw) and an Elscint Promeda Mössbauer multichannel analyzer operating in the multiscaling mode were used to accumulate unfolded spectra. The velocity scale was calibrated by using a standard iron-foil absorber and ⁵⁷Co/Rh source mounted on the reverse end of the transducer. Calibration spectra were thus recorded without interruption of the drive sequence. The calibration spectra were computer-fitted to give a linear velocity scale and folding point.

Folded ¹²⁷I spectra were fitted by using the program GMFP,¹⁵ which incorporates full-transmission integral procedures. These procedures require, among other things, the effective recoilless fraction of the source, the dimensionless absorber thickness of the sample, and the source line width, all of which are unknown parameters in this study. Consequently, the source line width was arbitrarily set equal to the natural line width, 1.27 mm s⁻¹, the dimensionless absorber thickness was made a variable parameter of the iterative fitting process, and the effective recoilless fraction was set at various fixed values until optimum agreement between the experimental and calculated spectra was obtained. The effective

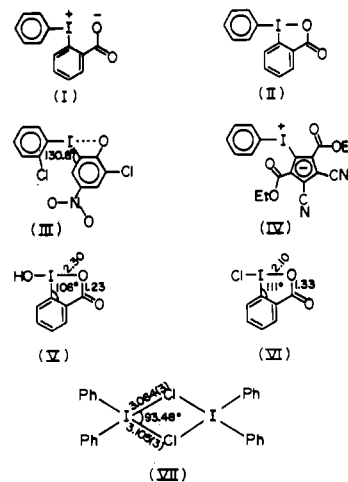
recoilless fraction of the source that gave the best agreement, when corrected crudely for the estimated background count rate and for the use of ¹²⁷I (57.6 keV), is of approximately the same magnitude as that reported for crystalline Ca₃^{129m}TeO₆ and Mg₃^{129m}TeO₆ (27.7 keV). Our estimate for amorphous Ca₃^{127m}TeO₆: $f_{129} = 0.75$ at 4.2 K; estimated from

$$f_{129} = \exp[(\ln f_{127})E_{\gamma 129}^2/E_{\gamma 127}^2]$$

Literature value for Ca₃^{129m}TeO₆ or Mg₃^{129m}TeO₆: $f_{129} = 0.82$ at 4.2 K.¹³

Discussion

Structure. The geometry about iodine consists of primary bonds to the phenyl rings of lengths 2.105 (4) and 2.119 (4) Å with a C-I-C angle of 95.2 (1)°. These two phenyl rings are almost perpendicular with an angle between their least-squares mean planes of 84.7°. In addition to the two I-C bonds, the iodine forms a weak bond of length 2.478 (4) Å with O(1) of the *o*-carboxylate group, which is virtually [0.024 (3) Å] in the same plane as ring C1-C6 and approximately trans [C7-I-O1 = 169.0 (1)°] to the I-C7 bond. Thus, the overall primary geometry of iodine is intermediate between tetrahedral AX₂E₂ with a strong face-capping I...O contact and trigonal-bipyramidal AX₃E₂ with I-O1 as an axial primary bond (Figure 1). Equivalently, the bonding description is intermediate between the zwitterionic form (I) and



the covalent benziodoxole form (II). By the use of the bond

(15) Ruebenbauer, K.; Birchall, T. *Hyperfine Interact.* **1979**, *7*, 125.

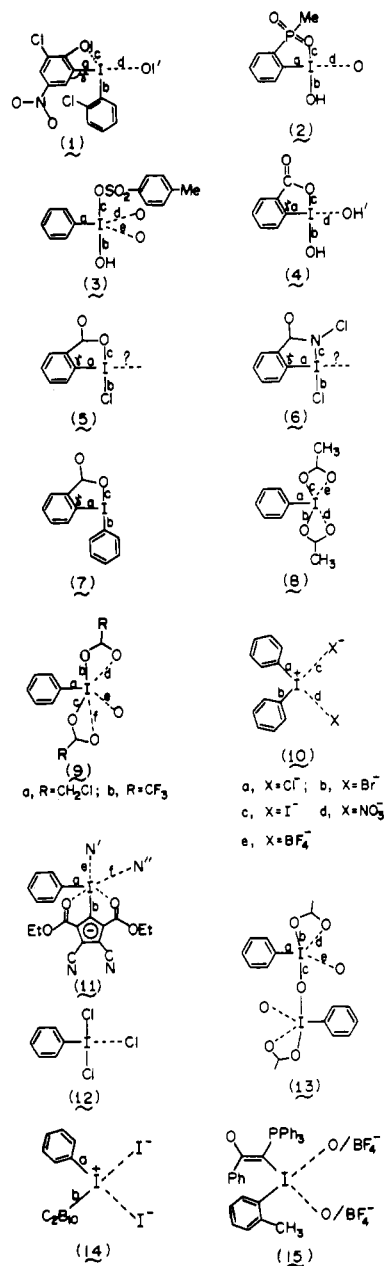
valence parameters of Troemel,¹⁶ the present I—O distance corresponds to a bond valence of 0.295 whereas the two I...O distances in diphenyliodonium nitrate¹⁷ (2.768 and 2.877 Å) correspond to a bond valence sum of 0.305.

In the trigonal-bipyramidal formulation, the "equatorial" I—C1 bond [2.119 (4) Å], which should nominally be shorter than the axial bonds, is slightly but significantly longer than I—C7 [2.105 (4) Å]. These bonds are slightly longer than the equatorial I—C bonds in $\text{PhI}(\text{OAc})_2$ ⁹ and $\text{PhI}(\text{OCOCHCl}_2)_2$ ⁹ [2.090 (6) and 2.083 (12) Å, respectively] but generally comparable to the I—C bond lengths in phenyl-9-*o*-carboranyliodonium iodide¹⁸ [2.111 (8) and 2.104 (8) Å] and in the diphenyliodonium salts with NO_3^- , Cl^- , Br^- , I^- , and BF_4^- counterions [2.071 (10)–2.114 (9) Å].^{17,19–21} The I—C bond length in 1,3-dihydro-1-hydroxy-3-oxo-1,2-benziodoxole [2.16 (5) Å] may be longer than those in the present compound.²² The length of I—C1 in the present compound may be partly due to the repulsive nature of the C7...H1 inter-ring contact [2.56 (4) Å], which is significantly shorter than van der Waals distances (ca. 2.95 Å).

The present C—I—C bond angle of 95.2 (1)° is significantly larger than C—I—C angles in the diphenyliodonium salts mentioned above [91.8 (6)–93.2 (5)°] but is smaller than the C—I—C bond angles in the (oxyphenyl)iodonium betaine (III)²³ [97.8 (4)°] and the related compound (IV)²⁴ [98.7 (2)°]. Increase in this angle may be due to an attempt to maximize the strength of the intramolecular contacts in III, IV, and the present compound and to reduce the C7...H1 contact above.

Inspection of the bonding in a variety of organoiodine(III) compounds (1–15) shows a large variation in I—O bond lengths in nominally AX_3E_2 trigonal-bipyramidal molecules from 1.940 (4) to 2.473 (3) Å (Table IV). Further I...O distances in these compounds, although common, are all longer than 2.768 (8) Å and can be considered to be secondary bonds. The directional preferences of these secondary bonds are such that either an interaction forms approximately trans to the equatorial bond and bisecting an E...E edge of the trigonal bipyramid (an $\text{AX}_3\text{Y}'\text{E}_2$ geometry) or two interactions occur approximately capping two XEE faces involving the axial ligands and the equatorial lone pairs (an $\text{AX}_3\text{Y}_2\text{E}_2$ geometry). Unexpectedly, apart from the intramolecular I—O1 bond/contact no further I...O contacts involving the oxygen atoms of the carboxylate group or water are observed in the present compound and the closest approaches trans to the equatorial I—C1 bond are ≥ 3.5 Å in length involving C5 and H4 of a glide-related molecule (Figure 2). The I...C5 contact [3.585 (4) Å] is slightly less than van der Waals limits (3.70 Å) but considerably longer than analogous I...O interactions. Instead, the crystal packing is dominated by hydrogen bonds [O1...H11 = 2.25 Å and O2...H12 = 2.03 Å] and interactions between the phenyl rings (Figure 2).

Other evidence for the attractive nature of the I—O1 interaction can be seen in the lengthening of C13—O1 to 1.272 (5) Å [cf. C13—O2 = 1.223 (4) Å] and some distinct distortions in the bond angles around C13, i.e. C6—C13—O1 = 115.2 (3)° and O2—C13—O14 = 125.2 (4)°. Other angular distortions at atoms C1—C6 from expected values are smaller in magnitude (Table III) and must partly be attributed to the effects of second- and



third-row elements on the internal bonding in phenyl rings²⁵ in addition to the I—O1 interaction. None of these angles are as large as the I—C—C angle of 130.8° in compound III, which has an intramolecular secondary I...O bond of 2.768 (8) Å, or as small as the internal I—C—C angles of 106 and 111° in the benziodoxole compounds V and VI. Similarly, the present C13—O1 bond is intermediate in length between the C—O intra-ring distances of 1.23 and 1.33 Å in V and VI (the I—O distances being 2.30 and 2.10 Å, respectively^{22,26}).

The present structure may be compared to some (*o*-formylphenyl)telluryl and -selenyl bromide compounds²⁷ in which intramolecular Te...O and Se...O interactions [of lengths 2.31 (2) and 2.31 (2) Å, respectively] with the *o*-formyl oxygen approximately trans to the Te(Se)—Br bonds result in a lengthening of the C=O bonds to 1.28 (3) and 1.25 (3) Å, respectively. Similarly, in a series of donor-acceptor complexes with AlCl_3 and SbCl_5 coordinated via C—O—M bridges, the C—O distances are

(16) Troemel, S. *Acta Crystallogr., Sect. C: Cryst. Struct. Commun.* **1985**, C41, S209 (Abstract 08-1-3).

(17) Wright, W. B.; Meyers, E. A. *Cryst. Struct. Commun.* **1972**, 1, 95.

(18) Ionov, V. M.; Subbotin, M. Y.; Grushin, V. V.; Tolstaya, T. P.; Lisichkina, I. N.; Aslanov, L. A. *Zh. Strukt. Khim.* **1983**, 24, 139.

(19) Struchkov, Y. T.; Khotsyanova, T. L. *Izv. Akad. Nauk SSSR, Ser. Khim.* **1960**, 821; *Chem. Abstr.* **1966**, 65, 11028g.

(20) Alcock, N. W.; Countryman, R. M. *J. Chem. Soc., Dalton Trans.* **1977**, 217.

(21) Khotsyanova, T. L.; Babushkina, T. A.; Saatsazov, V. V.; Tolstaya, T. I.; Lisichkina, I. N.; Semin, G. K. *Koord. Khim.* **1976**, 2, 1567.

(22) Shefter, E.; Wolf, W. *J. Pharm. Sci.* **1965**, 54, 104.

(23) Page, S. W.; Mazzola, E. P.; Mighell, A. D.; Himes, V. L.; Hubbard, C. R. *J. Am. Chem. Soc.* **1979**, 101, 5858. Hubbard, C. R.; Himes, V. L.; Mighell, A. D. *Acta Crystallogr., Sect. B: Struct. Crystallogr. Cryst. Chem.* **1980**, B36, 2819.

(24) Druck, U.; Littke, W. *Acta Crystallogr., Sect. B: Struct. Crystallogr. Cryst. Chem.* **1978**, B34, 3092.

(25) Domenicano, A.; Vaciano, A.; Coulson, C. A. *Acta Crystallogr., Sect. B: Struct. Crystallogr. Cryst. Chem.* **1975**, B31, 1630.

(26) Prout, K.; Stevens, N. M.; Coda, A.; Tazzoli, V.; Shaw, R. A.; Demir, T. Z. *Naturforsch., B: Anorg. Chem., Org. Chem.* **1976**, 31B, 687.

(27) Baiwir, M.; Llabres, G.; Dideberg, O.; Dupont, L.; Piette, J. L. *Acta Crystallogr., Sect. B: Struct. Crystallogr. Cryst. Chem.* **1974**, B30, 139; **1975**, B31, 2188.

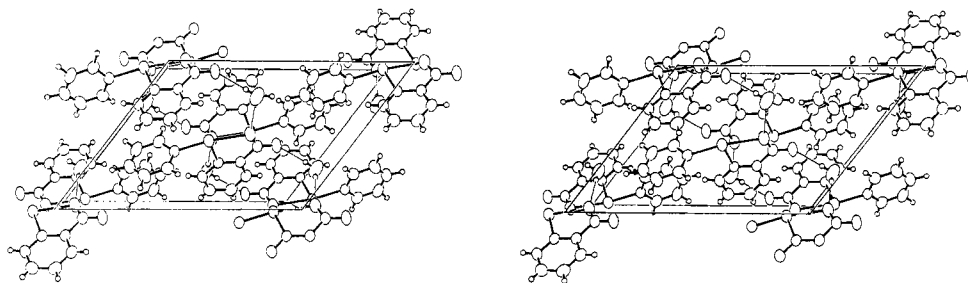


Figure 2. Stereoscopic view of the crystal packing down *b*.

Table V. ^{127}I Mössbauer Parameters for Organoiodine(III) Species

	isomer shift, ^a mm s ⁻¹	$e^2q^{127}Q_B/h$, MHz	η	Γ , mm s ⁻¹
Ph(<i>o</i> -CO ₂ C ₆ H ₄)I·H ₂ O ^b	-0.50 (3)	+1914 (6)	0.499 (6)	1.50 (4)
[Ph ₂ ICl] ₂ ^c	-0.54 (na) ^f	+2044 (19)	0.31 (2)	2.13 (13)
2,6-(CO ₂) ₂ C ₆ H ₃ I ^d	-0.67 (7)	+2585 (20)	0.92 (5)	na
PhICl ₂ ^d	-0.62 (5)	+2525 (30)	0.70 (5)	na
PhI(OAc) ₂ ^e	-0.87 (1)	+2507 (6)	0.79 (1)	1.53 (4)
PhIO ^d	-0.57 (5)	+2345 (20)	0.60 (5)	na
PhIO ^e	-0.51 (3)	+2410 (15)	0.47 (1)	2.08 (9)

^a Isomer shifts relative to I⁻. ^b This work. ^c Reference 10. ^d Reference 31. ^e Reference 30. ^f na = not available.

1.211–1.236 Å, all significantly less than the present C13–O1 distance.²⁸ Finally, in PhI(OAc)₂ the average C–O bond lengths are 1.312 (8) and 1.219 (9) Å to the primary and secondary bonded oxygen atoms [the corresponding I–O and I...O distances are 2.156 (5) and 2.833 (6) Å].⁹

The absence of any intermolecular I...O interactions in the present compound is unexpected but does show that in some compounds secondary bonds are energetically less favorable than hydrogen bonds in determining crystal packing. A similar observation has been made for the crystal packing of bis(4-hydroxy-3-methylphenyl)tellurium(IV) dichloride.²⁹ Note, however, that in 1,3-dihydro-1-hydroxy-3-oxo-1,2-benziodoxole both hydrogen and I...O secondary bonds determine the crystal packing.²²

Mössbauer Spectrum. The ^{127}I Mössbauer spectrum of C₆H₅IC₆H₄CO₂·H₂O is shown in Figure 3. The relative positions and intensities of the lines indicate a positive quadrupole coupling constant ($e^2q^{127}Q_B/h$) and asymmetry parameter (η) of 0.499 (6). The fitted parameters along with some literature data for related I(III) species are given in Table V. Iodine(III) compounds invariably display positive quadrupole coupling constants because the two nonbonding pairs of electrons on iodine are axially disposed to one another, imposing a negative electric field gradient at ^{127}I , which possesses a negative nuclear quadrupole moment. It has been noted¹⁰ that changes in the secondary interactions at iodine have only a small influence on the magnitude of the quadrupole coupling whereas changes in primary bonding have a much more significant effect. The present example bears this out in that its quadrupole coupling is comparable to those of the diphenyliodonium halides¹⁰ and considerably smaller than those of the monoorganoiodine(III) species.^{30,31} This, and the fact that the monoorgano species generally display larger asymmetry parameters, is a consequence of the greater contribution to the electron density in the *xy* plane about iodine by the C–I bonds than by the weaker bonds to the more electronegative elements, oxygen and halogens: the major or *z* axis of the EFG tensor is in the direction of the iodine lone pairs.

The most relevant comparison of the data in Table V is between the title compound and the diphenyliodonium chloride dimer (VII). The nearly identical isomer shifts for these two compounds indicate approximately equal withdrawal of valence p-electrons, $\sim 0.5 e^{31}$ from iodine by the ligands, assuming only p-orbital involvement

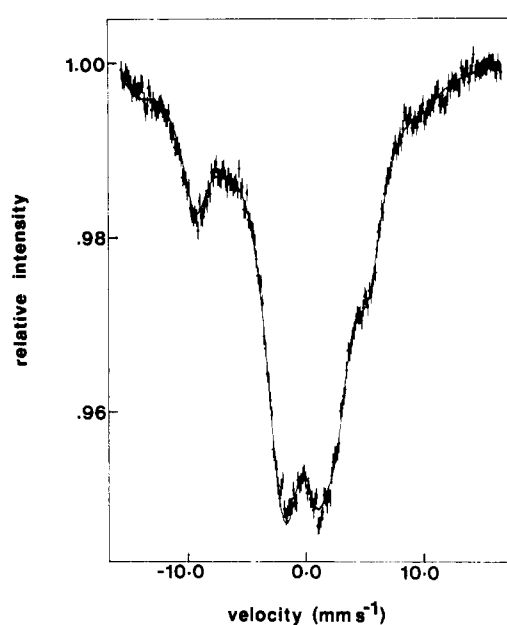


Figure 3. ^{127}I Mössbauer spectrum at 4.2 K of C₆H₅I(*o*-CO₂C₆H₄)·H₂O.

in the bonding. However, the difficulty of measuring precisely the ^{127}I isomer shifts and the relative insensitivity of these isomer shifts to electron configuration renders this only an approximation. Of more interest are the smaller quadrupole coupling constant and larger asymmetry parameter of the title compound. These facts are consistent with the I...O interaction contributing more electron density to the iodine *xy* plane in C₆H₅IC₆H₄CO₂·H₂O than the combined contribution by the two bridging chlorides in the diphenyliodonium chloride dimer. The asymmetry parameter of the title compound arises because of the complete lack of any secondary interaction with iodine in a direction opposite to C1. The smaller η value for [Ph₂ICl]₂ arises from a slight asymmetry in the I–Cl–I bridging distances.²⁰ That the asymmetry parameter for C₆H₅IC₆H₄CO₂·H₂O is not even larger than observed is a testament to the weak secondary nature of the I...O interaction.

Application of the Townes–Dailey model³¹ to the Mössbauer data, with the assumption of only p-orbital involvement in the bonding and no π -bonding, i.e. full *s* and *p_z* occupancy, implies an effective charge on iodine of +0.67 as compared to +0.78 for [Ph₂ICl]₂. The electron occupancies of the *p_x* and *p_y* orbitals are 1.30 and 1.03, respectively, for the title compound and 1.22 and 1.00 for [Ph₂ICl]₂. Presumably, the *x* directions are approximately

(28) Chevrier, B.; Weiss, R. *Angew. Chem., Int. Ed. Engl.* **1974**, *13*, 1.
 (29) Jones, R. H.; Hamor, T. A. *J. Organomet. Chem.* **1984**, *262*, 151.
 (30) Birchall, T.; Smegal, J. A.; Hill, C. L. *Inorg. Chem.* **1984**, *23*, 1910.
 (31) Ehrlich, B. S.; Kaplan, M. *J. Chem. Phys.* **1971**, *54*(2), 612.

parallel to the C-I-O near-linear moiety and the direction of the shorter of the two I-Cl interactions, respectively, for these two compounds. The difference implies an I-O bond order of 0.27, assuming that the two I-C bonds contribute equivalently to the I p_x and p_y orbitals, respectively. This compares well with the value of 0.295 derived from the interatomic separation discussed above. Such agreement, which may well be somewhat fortuitous in view of the assumptions implied, does suggest that further studies correlating bond valence parameters with Mössbauer data may help in the understanding of the nature and order of secondary bonds in iodine(III) and related species.

Acknowledgment. We thank the Natural Sciences and Engineering Research Council of Canada for providing operating grants (to T.B.) and an equipment grant for the diffractometer and Dr. J. W. Harvey and M. P. Butler of the McMaster Reactor Facility for help with the neutron irradiations.

Registry No. $\text{Ca}_3^{127}\text{TeO}_6$, 101419-02-7; TeO_2 , 7446-07-3; CaO , 1305-78-8; Ca_3TeO_6 , 20354-81-8; I_2 , 7553-56-2; diphenyliodonium-2-carboxylate hydrate, 96195-89-0.

Supplementary Material Available: Tables VI and VII, containing anisotropic thermal parameters and final structure factor amplitudes (15 pages). Ordering information is given on any current masthead page.

Contribution from the Laboratoire de Chimie de Coordination du CNRS, Unité No. 8241 liée par convention à l'Université Paul Sabatier, 31400 Toulouse, France, and School of Chemical Sciences, University of Illinois, Urbana, Illinois 61801

Manganese(II) Complexes of Polydentate Schiff Bases. 1. Synthesis, Characterization, Magnetic Properties, and Molecular Structure

Bouchra Mabad,^{1a} Patrick Cassoux,^{1a} Jean-Pierre Tuchagues,^{*1a} and David N. Hendrickson^{*1b}

Received September 17, 1985

The synthesis, infrared spectra, EPR, and variable-temperature magnetic susceptibility of 13 manganese(II) complexes with Schiff base ligands are described. These potentially penta- or hexadentate Schiff base ligands include N_2O_3 , N_3O_2 , and N_4O_2 donor sets and result from the condensation of salicylaldehyde, or 5-nitrosalicylaldehyde, with diaminopropanol or tri- or tetraamines. The crystal molecular structure of $\text{Mn}^{\text{II}}[\text{5-NO}_2\text{-sal-N}(1,5,9,13)] \cdot 0.65\text{C}_2\text{H}_4\text{Cl}_2$ has been established by X-ray diffraction methods. This complex crystallizes in the orthorhombic space group $D_{2h}^6\text{-Pnna}$ in a cell of dimensions $a = 20.732(4) \text{ \AA}$, $b = 16.906(2) \text{ \AA}$, and $c = 15.861(3) \text{ \AA}$, with $Z = 8$. The structure was solved by the heavy-atom method and refined by a full-matrix least-squares technique to conventional agreement indices $R = 0.038$ and $R_w = 0.041$ with 2208 unique reflections for which $F_o^2 > \sigma(F_o^2)$. The results obtained provide evidence that all manganese(II) complexes described here are high-spin penta- or hexacoordinated species. Minor changes in the design of the polydentate ligands result in different architectural arrangements of the corresponding complexes: $\text{Mn}^{\text{II}}(\text{saldpt})$ and $\text{Mn}^{\text{II}}(\text{5-NO}_2\text{-saldpt})$, characterized by the N_3O_2 ligand donor set with propylene units bridging the three N atoms, are monomeric. Also monomeric are $\text{Mn}^{\text{II}}(\text{salaep})_2$ and $\text{Mn}^{\text{II}}(\text{5-NO}_2\text{-salaep})_2$, both of which have two tridentate N_2O ligands, and $\text{Mn}^{\text{II}}[\text{sal-N}(1,4,7,10)]$, $\text{Mn}^{\text{II}}[\text{5-NO}_2\text{-sal-N}(1,4,7,10)]$, $\text{Mn}^{\text{II}}[\text{sal-N}(1,5,8,12)]$, $\text{Mn}^{\text{II}}[\text{5-NO}_2\text{-sal-N}(1,5,8,12)]$, $\text{Mn}^{\text{II}}[\text{sal-N}(1,5,9,13)]$, and $\text{Mn}^{\text{II}}[\text{5-NO}_2\text{-sal-N}(1,5,9,13)]$, which incorporate hexadentate N_4O_2 ligands. $\text{Mn}^{\text{II}}(\text{saldien})$, which has a N_3O_2 donor set ligand with ethylene bridges between the three nitrogen atoms, is a dimer. $\text{Mn}^{\text{II}}(\text{salprenOH})$, which has a N_3O_3 donor set ligand with an alcoholic function between the two imine nitrogen atoms, exhibits a structure with extended intermolecular magnetic exchange interactions in the solid state. $\text{Mn}^{\text{II}}(\text{5-NO}_2\text{-saldien})$ exhibits weak extended intermolecular interactions in the solid state and is a dimer when dissolved in noncoordinating solvents. IR and EPR data indicate the presence of cis and trans isomers with respect to the phenolic oxygen atoms for all monomeric complexes. The dimeric complexes behave as spectral analogues for the active site of the photosynthetic water-splitting enzyme.

Introduction

Manganese is of industrial and biological importance. Manganese(III) is known to oxidize alkylbenzenes, alcohols, carboxylic acids, phenols, and ethers.² The site where oxidation of water gives dioxygen in photosynthesis³ and the electron-transfer reaction of mitochondrial superoxide dismutase⁴ both involve manganese ions. The role that manganese plays in all these processes is undoubtedly related to the ability of the manganese ion to function as a redox catalyst.⁵ The capacity of the metal ion to change between oxidation states can be related to metal-metal interactions (binuclear and multi-metal-centered catalysts)⁶ and/or to the ligand field produced about the metal ion.⁷ Thus, the ligand

structure that maintains the metal centers in close or remote proximity and creates the ligand field plays a key role in the oxidation-state accessibility. In this regard, the oxidation-state accessibility of manganese has been explored by using a large variety of ligands.⁸

Very little is known about the role of manganese in photosynthetic systems. In green plants and algae, although manganese is known to be at the active site of a metalloprotein that mediates the oxidation of water to molecular oxygen, its exact role and environment in the thylakoid membrane are unknown.⁹ The stoichiometry requirement of manganese for O_2 evolution in active thylakoid membranes is four¹⁰ per center. The oxidation state of these manganese ions is thought to vary through the five Kok cycle states³ ($\text{S}_0\text{-S}_4$) between 2+ and 4+.⁹ EXAFS studies¹¹

- (1) (a) Université Paul Sabatier. (b) University of Illinois.
- (2) Benson, D. *Mechanisms of Oxidation by Metal Ions*; Elsevier: New York, 1976.
- (3) (a) Kok, B.; Forbush, B.; McGloin, M. *Photochem. Photobiol.* **1970**, *11*, 457-475. (b) Cheniae, G. M.; Martin, M. *Biochim. Biophys. Acta* **1970**, *197*, 219-239.
- (4) Fridovich, I. *Adv. Inorg. Biochem.* **1979**, *1*, 67-91.
- (5) (a) Calvin, M. *Rev. Pure Appl. Chem.* **1965**, *15*, 1-10. (b) Olson, J. M. *Science (Washington, D.C.)* **1970**, *168*, 438-446. (c) Keele, B. B.; McCord, J. M.; Fridovich, I. *J. Biol. Chem.* **1970**, *245*, 6176-6181.
- (6) Muetterties, E. L. *Bull. Soc. Chim. Belg.* **1975**, *84*, 959-986 and references therein.
- (7) Buckingham, D. A.; Sargeson, A. M. In *Chelating Agents and Metal Chelates*; Dwyer, F. P., Mellor, D. P., Eds.; Academic: New York, 1969.

- (8) (a) Lawrence, G. D.; Sawyer, D. T. *Coord. Chem. Rev.* **1978**, *27*, 173-193. (b) Coleman, W. M.; Taylor, L. T. *Coord. Chem. Rev.* **1980**, *32*, 1-31.
- (9) (a) Clayton, R. K. *Photosynthesis, Physical Mechanisms and Chemical Patterns*; IUPAB Biophysics Series; Cambridge University Press: Cambridge, 1980. (b) Govindjee. *Photosynthesis, Energy Conversion by Plants and Bacteria*; Academic: New York, 1982; Vol. 1. (c) Livornis, J.; Smith, T. D. *Struct. Bonding (Berlin)* **1982**, *48*, 2-44. (d) Amez, J. *Biochim. Biophys. Acta* **1983**, *726*, 1-12.
- (10) Yocum, C. F.; Yerkes, C. T.; Blankenship, R. E.; Sharp, R. R.; Babcock, G. T. *Proc. Natl. Acad. Sci. U.S.A.* **1981**, *78*, 7507-7511.
- (11) Kirby, J. A.; Robertson, A. S.; Smith, J. P.; Thompson, A. C.; Cooper, S. R.; Klein, M. P. *J. Am. Chem. Soc.* **1981**, *103*, 5529-5537.